ELSEVIER

Tectonophysics 349 (2002) 203–219

TECTONOPHYSICS

www.elsevier.com/locate/tecto

Integration of zircon color and zircon fission-track zonation patterns in orogenic belts: application to the Southern Alps, New Zealand

John I. Garver [a,*], Peter J.J. Kamp [b]

[a] *Geology Department, Olin Building, Union College, Schenectady, NY 12308-2311, USA*
[b] *Department of Earth Sciences, The University of Waikato, Private Bag 3015, Hamilton, New Zealand*

Received 1 May 2000; accepted 16 October 2001

Abstract

An exhumed crustal section of the Mesozoic Torlesse terrane underlies the Southern Alps collision zone in New Zealand. Since the Late Miocene, oblique horizontal shortening has formed the northeastern–southwestern trending orogen and exhumed the crustal section within it. On the eastern side, rocks are zeolite- to prehnite–pumpellyite-grade greywacke; on the western side rocks, they have the same protolith, but are greenschist to amphibolite facies of the Alpine Schist. Zircon crystals from sediments in east-flowing rivers (hinterland) have pre-orogenic fission-track ages (>80 Ma) and are dominated by pink, radiation-damaged grains (up to 60%). These zircons are derived from the upper ~10 km crustal section (*unreset FT color zone*) that includes the Late Cenozoic zircon partial annealing zone; both fission tracks and color remain intact and unaffected by orogenesis. Many zircon crystals from sediments in west-flowing rivers (foreland) have synorogenic FT ages, and about 80% are colorless due to thermal annealing. They have been derived from rocks that originally lay in the *reset FT color zone* and the underlying *reset FT colorless zone.* The reset FT color zone occurs between ~250 and 400 °C. In this zone, zircon crystals have color but reset FT ages that reflect the timing of orogenesis.

Keywords: Fission track; Zircon; Exhumation; Radiation damage; New Zealand

1. Introduction

One of the primary records of erosional exhumation of orogenic belts is the sedimentary detritus deposited in adjacent basins. In many cases, this detritus holds the most complete record of the evolution of exhumation because much of the crustal material in an orogenic belt has been stripped away and the surface exposures retain a memory of only part of the orogenic cycle (Garver et al., 1999a). To better understand erosional exhumation, a number of researchers have focussed on reading various aspects of the sedimentary record for clues as to the history of exhumation. One important recent advance is using detrital zircon in the sedimentary detritus to infer the thermal evolution of orogenic systems (i.e. Garver and Brandon, 1994a,b; Lonergan and Johnson, 1998; Carter and Moss, 1999; Garver et al., 2000 and references therein).

* Corresponding author. Tel.: +1-518-388-6517.
E-mail addresses: garverj@union.edu (J.I. Garver), p.kamp@waikato.ac.nz (P.J.J. Kamp).

0040-1951/02/$ - see front matter
PII: S0040-1951(02)00054-9

Whereas a number of common detrital minerals have been used in sedimentary provenance studies, none has received more attention than zircon ($ZrSiO_4$) because of its ubiquitous occurrence due to its resistance to destruction in sedimentary and metamorphic environments. What makes this history readable is that zircon commonly contains trace amounts of uranium and thorium that decay through several radiogenic processes, which change not only the parent/daughter ratio, but also mineral properties. These processes result in a variety of primary and secondary effects that are useful in understanding timing of crystallization, thermochronology, crystal lattice transformation, and color generation. The radioactive decay of uranium and thorium in a single detrital grain not only allows dating of thermal and crystallization events, but the radiation damage causes crystallographic changes and the generation of color. Whereas fission tracks are generated by fission of ^{238}U in zircon, much greater damage is caused in the crystal by the more common alpha decay (α-decay) of both uranium and thorium. The α-damage in a zircon is related to the generation of color in zircon as well as metamictization (transition from a crystalline to an amorphous state) (Fielding, 1970; Ewing, 1994).

Therefore, the low-temperature history of a zircon (<400 °C) is recorded in: (a) α-damage; (b) fission damage; and (c) color. In theory, all three of these effects can be used to evaluate the thermotectonic evolution of an orogenic belt. However, only fission-track (FT) dating can be easily applied to sedimentary zircons because the closure temperature is reasonably well known and the methodology for evaluating single grains is well established (see Garver et al., 1999a). Although α-damage in zircon holds much promise for future studies in thermochronology, too little is currently known about its thermal bounds and measurement of total accumulated α-damage is not routine (Nasdala et al., 2001). However, color accumulation in zircon, and its thermal stability, are fairly well known (Gastil et al., 1967), and it should be possible to integrate studies using both fission damage and color accumulation to gain a more robust understanding of the thermal structure of orogenic belts prior to their exhumation. In this paper, we use an example of detrital zircon from the Southern Alps collision zone of New Zealand to show how these two techniques may be integrated (Figs. 1 and 2). Zircons shed west off this system have fission-track ages and accumulated color that are reset due to orogenically driven exhumation.

2. The Southern Alps collision zone

The Southern Alps collision zone occupies the central portion of the Australia–Pacific plate boundary in South Island, New Zealand. The collision zone is about 400 km long, incorporating foreland basins to the west and piggyback basins to the east (Figs. 1 and 2; Kamp et al., 1992; Sircombe and Kamp, 1998; Beaumont et al., 1996). The Alpine fault is the intracontinental suture and the locus of most of the oblique displacement between the two convergent blocks.

Reset K–Ar and zircon FT ages indicate rapid and widespread cooling of the Southern Alps from about 10–12 Ma (Adams and Gabities, 1985; Kamp et al., 1989; Tippett and Kamp, 1993), which is inferred to be the time when the plate boundary became obliquely convergent and exhumation began. Since then, erosion of the continental basement in the orogenic belt has given rise to a comparatively simple outcrop pattern in which amphibolite-grade schist eastward through biotite and chlorite schist into prehnite–pumpellyite-grade graywacke. Geodynamic modeling has shown that the rates of rock uplift and erosional exhumation are major controls on the narrow width of the mountain belt in South Island (Beaumont et al., 1996).

FT studies in the Southern Alps demonstrate the timing, magnitude, and pattern of exhumation that has led to exposure of the crustal section. Zircon FT ages decrease across the Southern Alps towards the Alpine Fault, and these data define two sets of zircon reset and partial annealing zones (Kamp et al., 1989; Tippett and Kamp, 1993). The older zircon ages are located within the greywacke succession mainly east of the current drainage divide and relate to Cretaceous exhumation (Kamp et al., 1989; Kamp, 2001). Reset and partially annealed zircon FT ages in the Alpine Schist west of the Main Divide indicate that exhumation of the crustal section is mainly a Late Cenozoic feature. The reset zircon FT ages indicate rapid cooling from 8 Ma (south) to 5 Ma (north; Figs. 1 and 2).

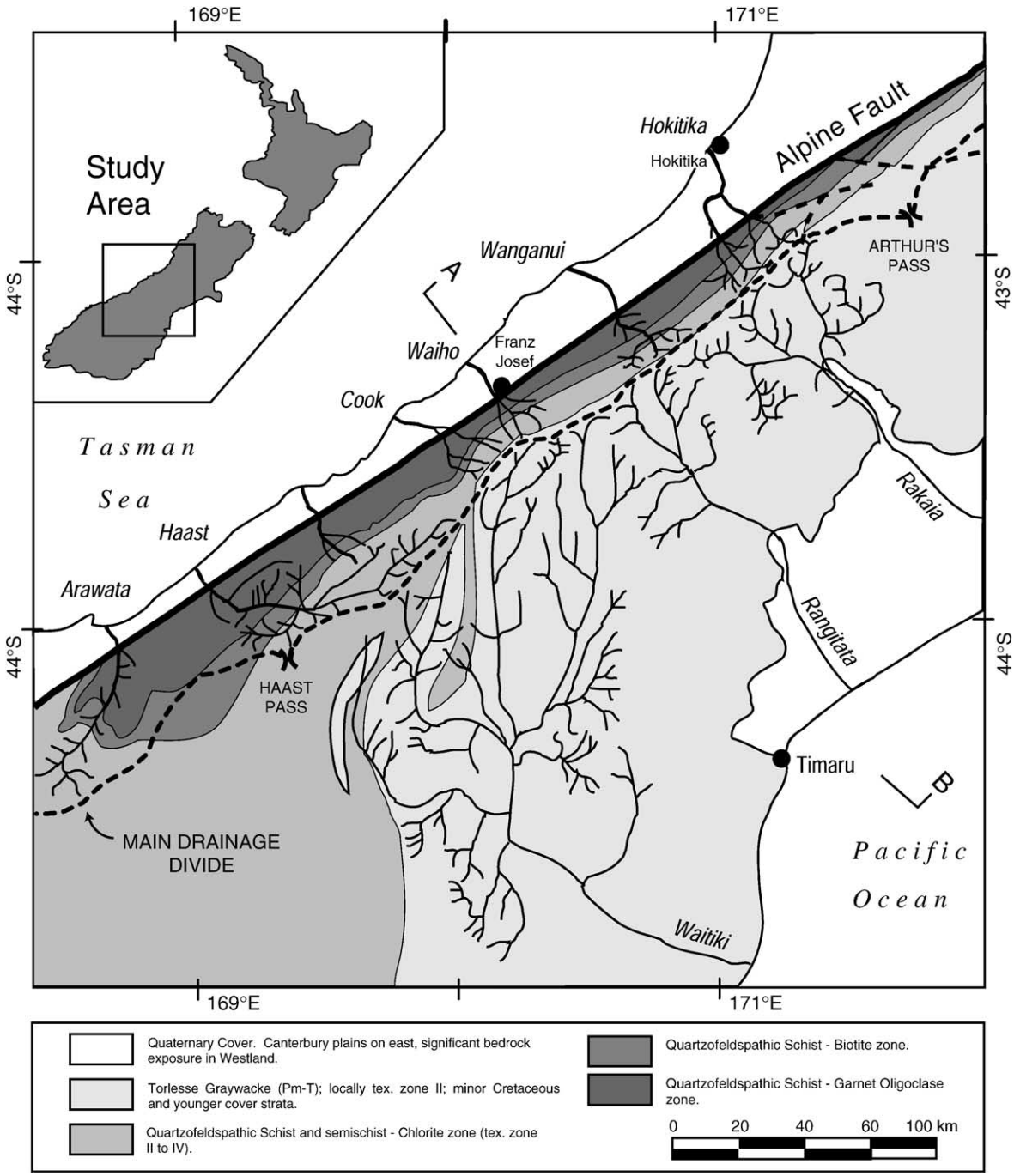

Fig. 1. Simplified geologic map of part of the South Island showing principal lithologies and drainages of the Southern Alps collision zone. Drainage divide of the Southern Alps is shown with a thick dashed line. Rivers that drain the western side have high gradients and mainly erode Alpine Schist; those draining the eastern side of the Alps have lower gradients, and almost exclusively erode graywacke of prehnite–pumpellyite grade.

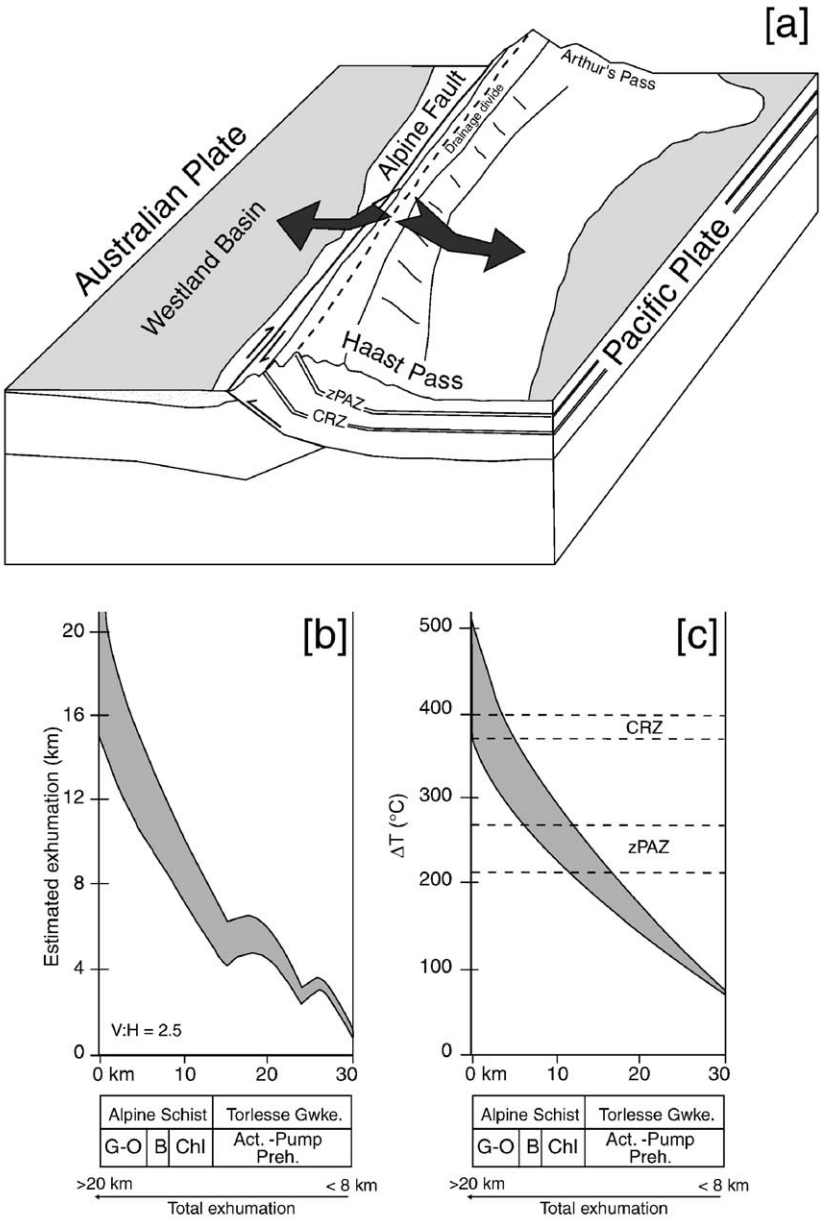

Fig. 2. Summary cartoon (a) of the uplift and exhumation of the Southern Alps and general constraints on the estimates of erosion (b) and cooling (c) within the orogen (modified from Kamp et al., 1989). Note the increase in amount of cooling and exhumation with increasing proximity to the Alpine Fault. ZPAZ is zircon partial annealing zone. CRZ is Color Removal Zone.

Interpretation of FT data across the Southern Alps has allowed mapping of the amount and pattern of Late Cenozoic exhumation, which increases from 2 to 18 km across the Southern Alps (Tippett and Kamp, 1993) (Fig. 2b). The modern drainage divide runs along the highest topography in the Southern Alps.

3. Radiation damage in zircon

Radiation damage in zircon results in metamictization and the generation of color over time. The following discussion includes establishing typical uranium and thorium concentrations in zircon, the occurrence of α-damage and fission damage, how radiation damage causes metamictization, and how radiation induces color change in zircons.

3.1. Uranium and thorium content of natural zircons

The concentrations of uranium and thorium in zircons are important in this discussion about radiation damage for several reasons. First, α-decay is common in all uranium and thorium isotopes, but only ^{238}U contributes significantly to fission damage. Second, uranium concentration limits what grains are datable by the FT method, thereby restricting our ability to date the thermal history of some grains (Fig. 3). Third, uranium and thorium concentrations bear on the generation of color as these elements progress though their α-decay series. Because α-decay results from both uranium and thorium, we use the notation in which U + Th (mainly ^{238}U, ^{235}U, and ^{232}Th) is represented by "eU" or "effective uranium" concentration (i.e. Gastil et al., 1967; Fig. 3).

Typical concentrations of uranium and thorium in all zircons fall between 5–4000 ppm for uranium and 2–2000 ppm for thorium, but some crystals are strongly zoned (see Speer, 1980). Our compilation suggests that typical natural detrital zircons have a mean of ~ 419 ppm U, and a mode of ~ 140 ppm U (see Fig. 4). Like uranium, natural thorium concentrations in zircon vary tremendously between crystals (Speer, 1980). To estimate typical thorium concentrations in zircon, we compiled data from U–Th–Pb Ion Microprobe studies of detrital zircon of different ages which suggests that the average Th/U ratio is 0.5 with a mode of about 0.4 although this estimate (and

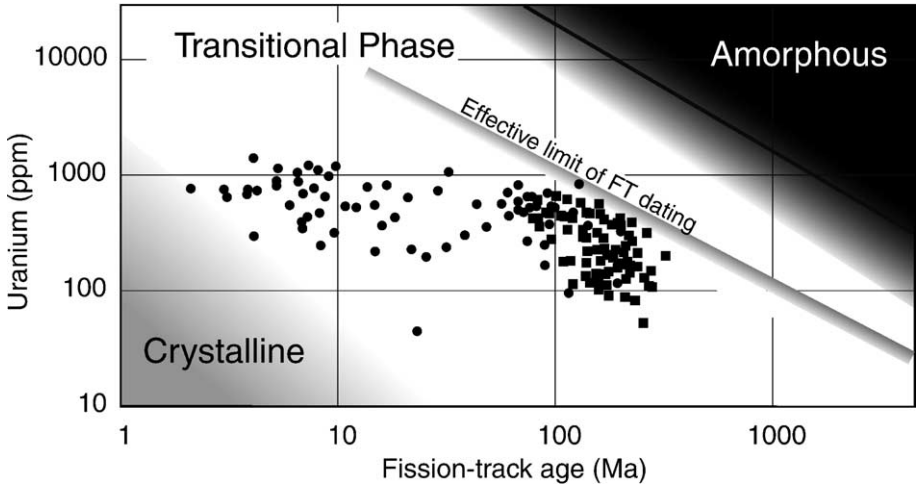

Fig. 3. Relationship between accumulated α-damage and fission-track damage in zircon. For both lines, uranium refers to the effective uranium (eU) that contributes to decay. For α-damage, eU includes decay from α-decay of ^{238}U, ^{235}U, and ^{232}Th, and for fission damage only ^{238}U. The upper solid line (in the "amorphous" field) represents the α-dose for the approximate onset of full metamictization or amorphization in zircon, which corresponds to about 0.5 displacements per atom (DPA) (see equation in Ellsworth et al., 1994). Note that the upper line showing the onset of metamictization corresponds to ~ 5×10^{15} α-decay events/mg, which is the general range of full metamictization (see Chakoumakos et al., 1987; Woodhead et al., 1991). FT dating is effectively limited to the lower two thirds of the transitional phase and the crystalline phase (below "effective limit of FT dating"). The circles represent FT ages from zircon from the Hokitika River, and the squares from the Rangitata River. The lower shaded region represents the range of damage that effectively results in a fully crystalline zircon ($< 10^{12}$ α-decay events/mg): grains in this region are difficult to routinely date using the detrital FT method because they have very low track densities and they require very long etch times (Garver et al., 1999b).

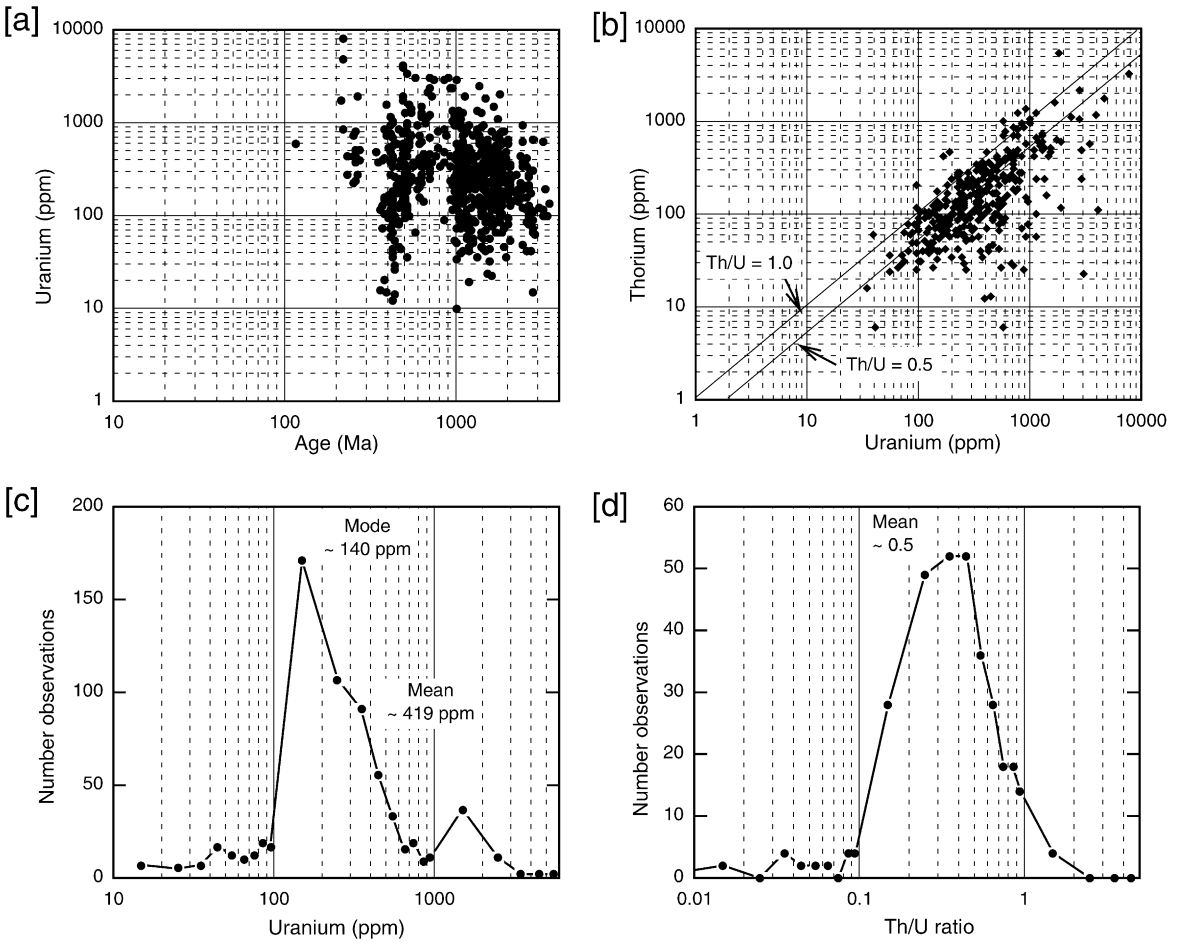

Fig. 4. Graphs showing the relationship of uranium and thorium content and age in natural detrital zircon grains. (a) Calculated U and apparent U/Pb age of 679 detrital zircon grains from various studies in the literature. All ages, whether concordant or discordant, are plotted are based on $^{206}Pb/^{238}U$ ratios unless noted otherwise below. Data used in the calculation of mean concentrations are from the following sources: Zhao et al. (1992; $n=63$; grain 22.1 excluded); Smith and Gehrels (1994, $n=54$); Miller and Saleeby (1991, $n=22$); Scott and Gauthier (1996, $n=19$): Gehrels and Dickinson (1995, $n=156$); Gray and Zeitler (1997, $n=66$); Roback and Walker (1995, $n=27$); Schäfer et al. (1995, $n=7$); Gehrels et al. (1996, $n=89$, only detrital units included); Rainbird et al. (1997, $n=54$). (b) Uranium vs. thorium for U–Th–Pb determined ages as determined from Ion Microprobe (SHRIMP dating). Data from Ireland (1992), Zhao et al. (1992), Schäfer et al. (1995), Gray and Zeitler (1997). (c) Frequency of uranium concentrations of single grains. Excluding one outlying data point (see "a" above), the mean uranium concentration is 419 ppm ($\pm$ 605 ppm) with a mode of 140 ppm. (d) Frequency of Th/U ratios from single zircon grains.

the uranium estimate above) may be slightly biased toward preselected grains (Fig. 4).

3.2. α–damage and fission damage

As uranium and thorium decay, α-damage and fission damage accumulate in zircon provided the crystal stays below the respective annealing temperatures, which fall between 200 and 300 °C (Fleischer et al., 1975; Tagami et al., 1996). α-Damage results in complex damage in a crystal, but two main types of damage are inferred (see Ellsworth et al., 1994). The first is minor disruption caused by α-particles, which dissipate energy by electronic excitation and ionization. The second, generally referred to as α-recoil damage, results from the heavy α-recoil nucleus which

dissipates energy by elastic collision (Holland and Gottfried, 1955; Murakami et al., 1991; Ellsworth et al., 1994; Ewing, 1994; Weber et al., 1994). Collectively, this "α-damage" results in significant atomic displacements and ionization in a zircon crystal.

Metamict zircons ("malacon," "low," or "γ" zircon) have accumulated severe radiation damage and as such there has been a significant change in color, density, and optical properties (Deer et al., 1982; Speer, 1980). In general, radiation damage that leads to metamictization is principally attributed to α-decay, which lowers the density of the zircon over time (Holland and Gottfried, 1955). One criteria for metamictization is the point at which the zircon becomes X-ray amorphous, which is an α-dose of approximately 2.0 to 8.0×10^{15} α-events/mg (~ 0.15 to 0.60 displacements per atom; Chakoumakos et al., 1987; Woodhead et al., 1991; Weber et al., 1994). To illustrate the relationship between age and metamictization, we show calculated α-damage for metamict zircon (upper line; Fig. 3) as well as the effective limit of track densities datable by the FT method (lower line; Fig. 3). In this plot, the general trend that high eU grains become metamict sooner than low eU grains can be clearly seen.

3.3. Zircon color

Zircon occurs in many colors including colorless varieties. Commonly reported colors include various shades of pink, red, purple, yellow, orange, brown as well as less common shades of green, and blue (Speer, 1980; Deer et al., 1982). However, most zircons fall into two general color series of increasing radiation damage: (a) a common pink series that ranges between pink, rose, red, purple ("hyacinth"), and black; (b) a less common yellow series that ranges between pale yellow, straw, honey, brown, and black (Gastil et al., 1967). These colors are related to trace-element composition and radiation damage. For some time, workers have linked color to total radiation damage (i.e. Hutton, 1950; Tomita and Karakida, 1954). Whereas the nuclear reactions giving rise to α-decay and fission decay are well known, the specifics of color generation are not.

Given the proper composition, zircons gradually accumulate color through electron displacements driven by the α-decay of uranium and thorium. Progression through the pink–red series is inferred to be related to: (a) time since cooling; (b) concentration of uranium and thorium; and (c) heavy rare earth element (HREE) content. At near-surface temperatures, zircons with typical compositions accumulate significant color only after 100s of millions of years (i.e. Nerurkar et al., 1979). The particular role of HREE in color generation in zircon is poorly understood, but europium may play a key role (i.e. Fielding 1970; Gaudette et al., 1981). Even with negligible radiation damage, color can be attained if the zircon has high overall REE concentrations. This crucial point underscores the need for future studies aimed at quantifying color, radiation damage, and crystal-specific chemistry. Zircons from felsic melts are typically richer in the REE and uranium, suggesting that they may accumulate color more quickly than other sources (Poldervaart, 1955, 1956; Speer, 1980). Future studies should be aimed at linking crystal-specific chemistry with total radiation damage to color attained.

3.4. Definition of the color removal zone

The removal of color in zircon has been observed in a number of crustal sections that show progressive metamorphism of rocks. These instances show color removal between: (a) green to brown biotite zones, (b) biotite/garnet to staurolite/sillimanite zones; and (c) biotite to staurolite zones (Gastil et al., 1967; Kodymová, 1977), indicating that color removal occurs between ~ 350 and 400 °C. By implication, a modern Color Removal Zone (CRZ) should occur at depth in the crust, below rocks that reside at 350 to 400 °C. In this definition, we include the partial color removal zone, which would include the higher part (low temperature) of the crustal section.

A few studies have quantitatively addressed the removal of zircon color under laboratory conditions, but it is clear that more studies are needed. The best experiments that we are aware of are those Gastil et al. (1967) in which pink zircons were heated for < 1 to 100 h in an oven. After heating, the "percent color retained" was visually estimated. Their results show that color annealing has a temperature range of ~ 325–475 °C and nearly full color removal (50% to 90%) occurs between ~ 350 and 430 °C for heating times of 10 to 100 h. Gastil et al. (1967) concluded that color loss is primarily a function of

maximum temperature rather than thermal duration. These studies suggest that color removal (annealing) at laboratory and geological time scales occur at about the same temperature, which may suggest that the kinetics of the process are controlled by high activation energies.

Despite the temperature range over which partial zircon color annealing occurs, it will be a narrow zone that occurs at depth in crustal sections. It is analogous to the modern apatite fission-track partial annealing zone (PAZ). The degree of development of a Color Removal Zone (CRZ) will be dependent upon zircon composition, particularly abundance of the elements causing radiation damage (U + Th) and those implicated in color generation (HREE). Because of variations in zircon composition, the zone will necessarily be physically defined by analysis of a multitude of crystals from a horizon.

3.5. Integration of zircon fission track and zircon color annealing signals

The combination in the one mineral phase (zircon) of two parameters (FT age and color) that have thermal stability at different temperature ranges opens up the potential to stratify an exhumed crustal section into a number of layers and assign paleotemperatures and/or age to transitions. Fig. 5 illustrates this concept for the Southern Alps collision zone. First, we discuss the temperature bounds of the zircon fission-track partial annealing zone.

While the temperature limits of the ZPAZ at geological time scales are known, in general, there is no agreement in details. The difficulty arises because the temperature at the base of a modern ZPAZ has not been measured directly; it likely lies above 255 °C (see Coyle and Wagner, 1996). A kinetic model based on laboratory-scale zircon annealing experiments, fitted to several borehole zircon FT data sets, predicts a temperature of about 310 °C at the base of a ZPAZ (Tagami et al., 1998). The temperature at the top of the ZPAZ lies above (hotter than) 200–210 °C based on the zircon FT ages and lengths at the base of the Vienna Basin borehole (Tagami et al., 1996) and Kola Peninsula hole SG-3 (Green et al., 1996). The fitted kinetic model of Tagami et al. (1998) suggests a temperature close to 210 °C for the top of the ZPAZ for 10^7 years time scale of heating.

Brandon et al. (1998) consider that these upper and lower (210–310 °C) bounds for a ZPAZ are too high,

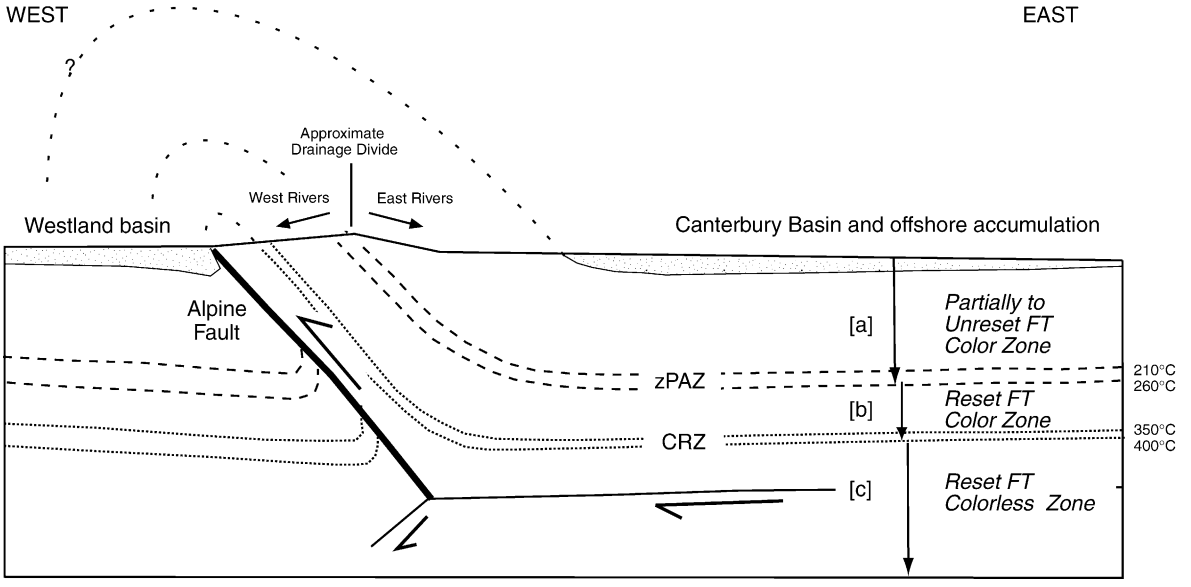

Fig. 5. Schematic cross-section modified from Beaumont et al. (1996) showing the broad crustal structure, nature of uplift and exhumation across the central part of the Southern Alps collision zone. Shown on the cross-section are the three zones defined by integration of the zircon FT thermochronometer and the zircon color thermometer, and the approximate temperatures of the transitions.

being closer to 180–240 °C for 10^7 years of heating. These estimates represent 10% and 90% annealing isopleths (strictly not the top and bottom of a PAZ), and are assigned to the component of zircon grains having the youngest FT ages in their samples, considered to be those which had the greatest amount of radiation damage and most susceptibility to annealing. This assignment is based on the fact that the thermal stability of fission tracks in zircon decreases with increasing α-damage (Kasuya and Naeser, 1988). Together, these points suggest that the temperature limits of a ZPAZ are dependent upon the time–temperature history of the sample host rocks, the degree of radiation damage contained in the crystals on entering the PAZ, and whether or not the stratigraphic/structural extents of fossil PAZs are picked from the central ages for samples or from a subset (least thermally stable) of the dated grains within samples. For example, in the rocks underlying the Southern Alps in which the detrital zircons will have accumulated radiation damage, the high end of the temperature limit for the ZPAZ is taken as 260 °C and the low end is taken as 210 °C.

Application of the zircon FT thermochronometer and the zircon color thermometer to samples from an exhumed crustal section potentially allows subdivision into numerous crustal layers. We can subdivide the crustal section into three layers (Fig. 5): (i) an upper *unreset FT color zone* (uFTCZ) with colored zircons carrying old ages (this includes the ZPAZ and above); (ii) a *reset FT color zone* (rFTCZ) in which FT ages are reset, but zircons retain color; and (iii) a *reset FT colorless zone* in which FT ages are reset and zircons are colorless. All three zones/layers will be

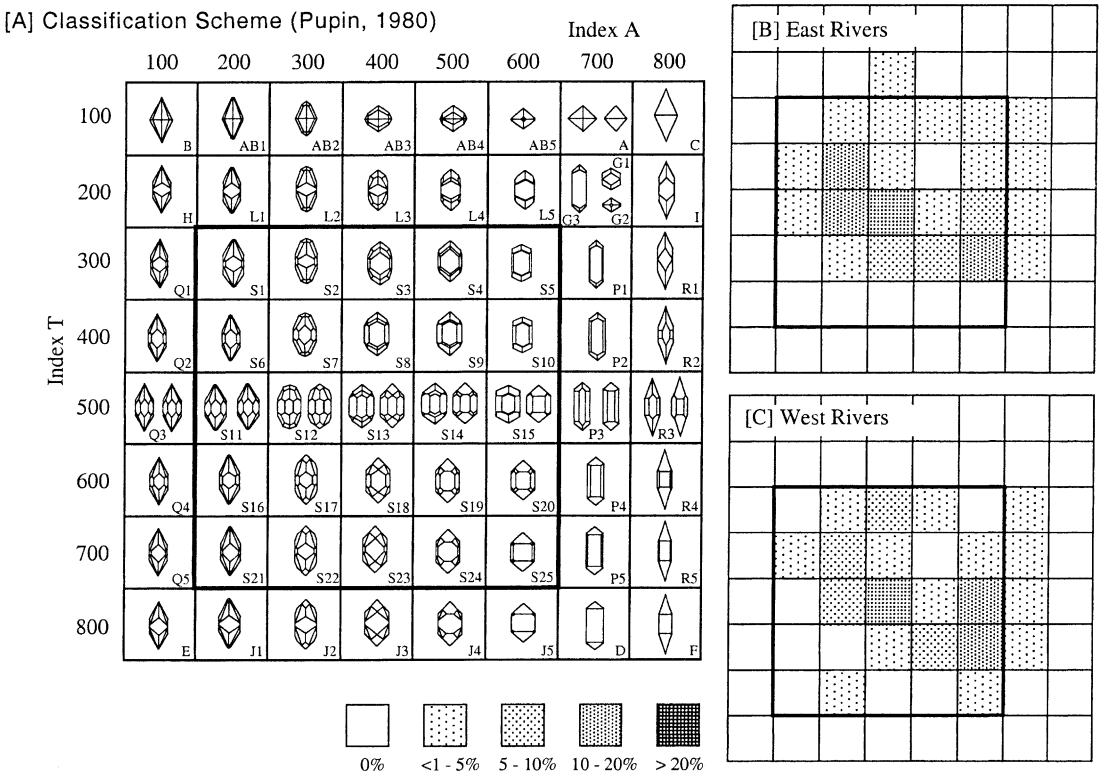

Fig. 6. Classification of zircon tracht and habit (see Pupin, 1980) and the results of (A) classification of detrital zircon from the east side (B) and the west side (C) of the Alps. For each figure, about 150 grains from all representative rivers studied (about 25 to 30 grains per river—see Table 1) were classified and then plotted.

distinctive and mapable along and across exhumed orogens through the combined use of the two parameters of zircon FT age and color.

4. Methods

Samples were collected from sand and gravel bar deposits with a gold pan near the center of riverbeds during low-discharge conditions. Concentrates were dried, and the zircons were separated using standard heavy liquid techniques. For topological analysis, a split fraction of zircon was mounted in epoxy on a glass petrographic slide. One-hundred individual zircons along parallel traverses were then evaluated for crystal habit, length, breath, and inclusions using transmitted light. Results are plotted and evaluated using standard techniques (see Fig. 6; see Pupin, 1980).

For color, loose zircons were point counted using reflected light. We used the following color categories: colorless, colorless with inclusions, gray, pink, rose, hyacinth, and yellow brown (Table 1). Note that once zircons are mounted in Teflon® (for FT analysis, see below), it is difficult to distinguish color. Future studies should strive to link color and FT age by hand picking suites, or some other means.

For FT dating, we used standard techniques for the external detector method of FT analysis of detrital zircon (see Table 1 and Garver et al., 1999b). We used the *Multi-Mount technique* which optimizes the total range of countable grains by ensuring that all grain populations are suitably etched by etching several mounts for different times (15, 30, and 60 h) and counting grains from each mount (see Table 2 and Fig. 7; Naeser et al., 1987 cf. to the multi-etch technique of Hasebe et al., 1993; Garver et al., 1999b). We use probability density (PD) plots to evaluate grain-age distributions (Fig. 7) (Brandon, 1996). Once constructed, these PD plots are then decomposed into individual component populations using a binomial peak-fitting method (Brandon, 1996; P1, P2, etc., on Fig. 7).

5. Results

Here, we evaluate the characteristics of zircons shed to either side of the orogenic belt. In doing so, we ask whether the fission-track ages and the color of

Table 1
Zircon color in major rivers draining the Southern Alps collision zone

River	Field no.	Colorless			Yellow brown	Red series		Series totals			*n*
		Clear	Inclusions	Gray		Pink	Rose	Red	Yellow	Colorless	
West-draining rivers											
Hokitika	97-6	54.8	21.2	2.9	2.9	18.3	0.0	18.3	2.9	78.8	104
Wanganui	97-8	79.8	5.8	10.6	1.9	1.9	0.0	1.9	1.9	96.2	104
Waiho	97-9	50.0	19.7	13.6	6.1	10.6	0.0	10.6	6.1	83.3	132
Haast	97-12	19.3	12.7	25.9	2.4	3.6	36.1	39.8	2.4	57.8	166
Arawata	97-11	67.9	0.0	14.5	8.4	8.4	0.8	9.2	8.4	82.4	131
Average		54.4	11.9	13.5	4.3	8.6	7.4	16.0	4.3	79.7	
East-draining rivers											
Tasman	97-13	43.0	4.7	0.0	7.5	35.5	9.3	44.9	7.5	47.7	107
Rangitata	97-17	31.5	1.9	1.9	8.3	38.9	17.6	56.5	8.3	35.2	108
Rakaia	97-19	47.6	1.9	1.0	14.6	22.3	12.6	35.0	14.6	50.5	103
Wilberforce	97-22	30.7	0.0	2.4	26.0	30.7	10.2	40.9	26.0	33.1	127
Average		38.2	2.1	1.3	14.1	31.9	12.4	44.3	14.1	41.6	

Shown are percentages in each category. Zircons point counted along a random traverse on a glass petrographic slide using an Olympus Binocular microscope. Rose is a "darker" pink but, in this case, include a few hyacinth grains (purple). Inclusions are large needles and included minerals. Inclusions occur in colored zircon, but were not noted. Gray zircons are included in the colorless suite because they lack shades of yellow or red.

Table 2
Zircon FT peak ages for modern river sediments, Southern Alps, New Zealand

Unit	Age	*n*	P1	P2	P3	P4
(a) Rangitata	0 Ma	75	101.9 Ma (− 4.4 + 4.6) 17.2%	153.8 Ma (− 5.2 + 5.3) 45.4%	222.2 Ma (− 7.3 + 7.5) 37.4%	
(b) Hokitika	0 Ma	75	6.5 Ma (− 0.3 + 0.3) 40.7%	21.2 Ma (− 1.1 + 1.1) 18.7%	73.0 Ma (− 2.3 + 2.4) 31.8%	148.8 Ma (− 9.2 + 9.8) 8.8%

Grain ages were determined using the standard techniques for the external detector method of detrital zircon (see Garver et al., 1999b). All binomial peakfit ages give at 1σ. Zircons from single samples were embedded into three separate 2 × 2 cm PFA Teflon® mounts at 330 °C. These mounts were then cut using 800 grit wet sandpaper, then polished using 3 and 1 μm diamond paste, and then finished using a 0.3 μm Al_2O_3 slurry. Each mount was etched different times to optimize countable grains (see Naeser et al., 1987; Garver et al., 1999b). Etching was done in nonreactive Teflon® dishes at 230 ± 2 °C in a thermostatically controlled oven. Mounts were continuously etched for 15, 30, and 60 h in a NaOH:KOH eutectic mixed with a ratio of 11.5:8.2. Etched mounts were cleaned in dilute HF for 15 min, rinsed, dried, and then freshly cleaved low-uranium mica flakes were affixed to the mounts. The samples were then irradiated at the Oregon State Nuclear Reactor with a nominal fluence of 2×10^{15} neutrons/cm^2. Uranium-doped glass standards (CN-1) were placed at either end of the sample stack to monitor fluence during irradiation, and from these glasses, a gradient was calculated and interpolated values were used in age calculations. Twenty-five random, but countable grains in a traverse, were counted for each of six mounts and the results were combined for this analysis. Samples were counted using a Zeiss Axioplan microscope with a magnification of 1250 × (50 × dry objective, 10 × oculars, 2.5 × tube factor). We used the zeta calibration approach in calculating ages with a zeta factor of 133.58 ± 1.1. Peak ages were calculated using a binomial statistical analysis (see Brandon, 1996). The number of grains in each analysis is represented by *n*. For full grain, age distribution data may be obtained from, http://zircon.union.edu/FT/tectonophysics_data.

zircon can be interpreted together to gain additional insight into the thermal structure of the exhumed crust. Before we make these interpretations, we need to address the following questions: (1) Are we assured that the zircons from both the east and the west represent similar populations with different thermal histories?; (2) Are the populations from the east and the west significantly different in terms of color?; and (3) Do the populations in the east and the west have different FT cooling ages?

5.1. Similarity of zircon populations

In light of previous work, it seems probable that the Alpine Schist is the mid to lower crustal equivalent of the upper crustal Torlesse greywacke. This correlation would be supported if zircon topology is similar between the units on either side of the Main Divide. Typological studies of zircon have been applied in petrogenetic analyses of zircon-forming environments (i.e. Pupin, 1980). Because zircons in both the east- and west-flowing rivers lack overgrowths, they provide information about the original Permo-Triassic (-Jurassic) provenance of the sediments. The population encompasses a variety of subtypes, but subtypes from individual rivers are indistinguishable (Fig. 6). Samples from both the east and west sides are similar, having a dominance of subpopulations around type S with a secondary occurrence of type P. Abundant in both suites are subtypes S7, S12, S13, S15, S20. Additionally, P1, P2, P3, P4 are not abundant, but are present in all samples. Therefore, zircon habit, combined with our observations of roundedness, and lack of overgrowths, suggest that zircons on either side of the orogen have a similar provenance, which reflects the original source of the Torlesse Terrane (e.g., Ireland, 1992; Pickard et al., 2000).

5.2. Color of zircon shed off the Southern Alps

West-draining rivers, which cut into biotite- and garnet-grade schist, are rich in colorless zircon. East-draining rivers, which cut into Permo-Triassic (-Jurassic) greywacke and drain into the Pacific Ocean, are rich in pink zircon. Some 50% to 70% of the zircons shed to the east are colored (pink, rose, or yellow) compared to ~ 20% shed to the west (Table 1). The differences in the color proportions of zircons shed to the east and those shed to the west reflect erosion from different crustal levels. The Garnet-Oligoclase Zone and the Biotite Zone underlie most of the western drainages and, therefore, these rocks experienced sufficient temperatures to anneal color in zircon.

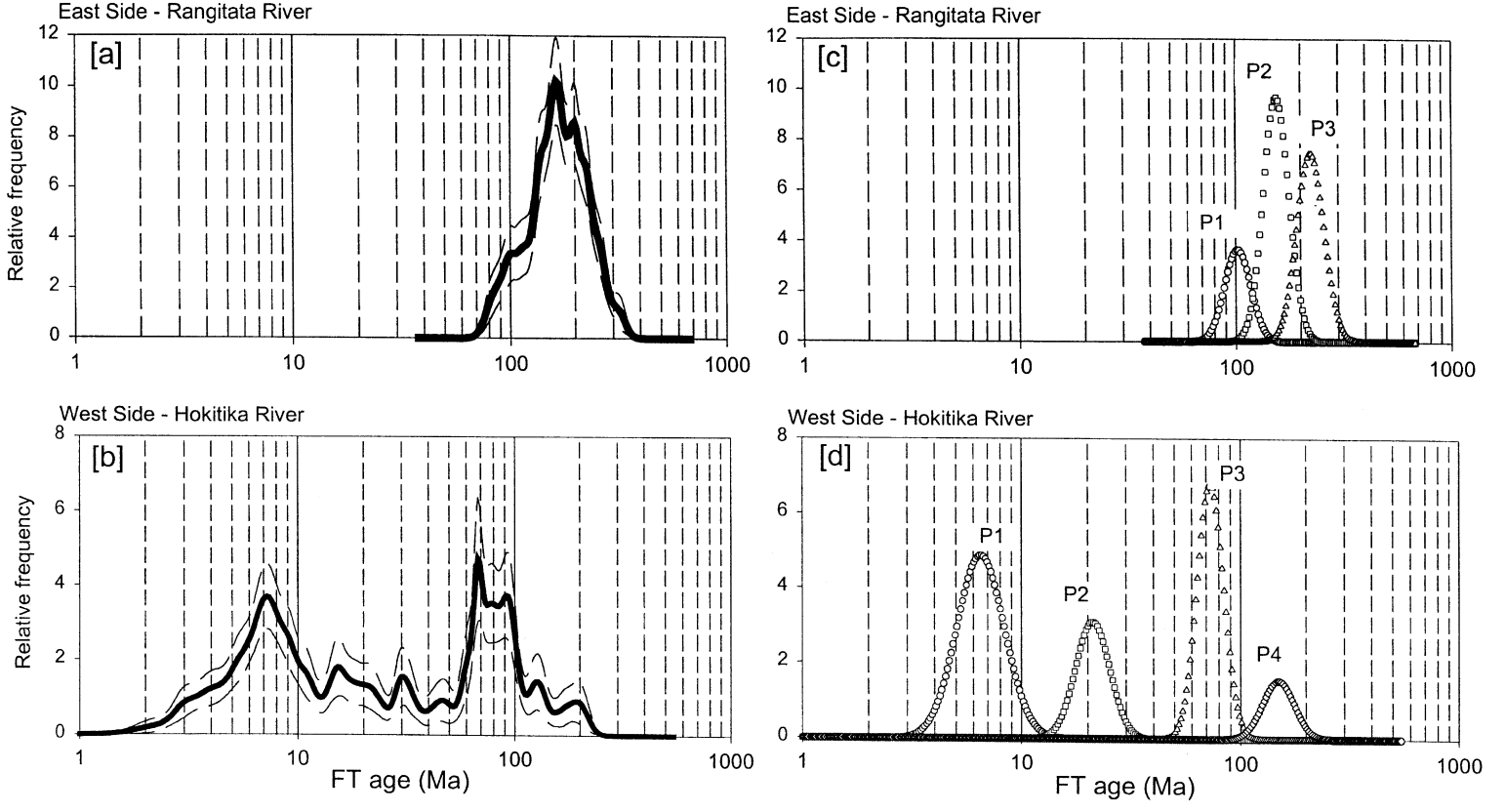

Fig. 7. Fission-track grain age (FTGA) distribution of detrital zircon shed from the Southern Alps (see Table 2 for explanation). (a) Probability Density (PD) plot of fission-track ages and 95% confidence interval from the Rangitata River (east side); (b) PD plot and 95% confidence interval from the Hokitika River (west side); (c) fitted binomial peaks for the Rangitata River; (d) fitted binomial peaks for the Hokitika River. Note that most FT grain ages shed to the west in a foreland position (Hokitika) are reset and record the young thermotectonic events associated with the collision represented by the Southern Alps. FT ages of zircon shed to the east, in a piggyback position to the orogenic system, are relatively old (none less than about 90 Ma) (see summary in Table 2).

The high proportion of colored zircons in east-flowing rivers reflects the fact that the source rocks remained below temperatures required to anneal color-induced radiation damage. Although the eastern rivers are rich in colored zircons, colorless zircons also exist. These colorless zircons (< ~ 40%): (a) are too young to have accumulated significant radiation damage given their eU; (b) have insufficient REE contents; or (c) have both low damage and low REE. In fact, it would be unusual for a mixed suite of detrital zircon in Mesozoic or younger sediments to be entirely colored for these reasons. U–Pb single-grain age data (Ireland, 1992) show that about half the dated zircons are Permian–Triassic and the other half are older, which is similar to our observed distribution of about 60% colored (i.e. old, or presumably pre-Permian or older radiation damage in this case) and about 40% colorless (i.e. Permian–Triassic).

Rivers that drain to the west are principally underlain by rocks of the Garnet-Oligoclase and Biotite Zones as well as minor lower grade Chlorite Zone rocks (Textural Zone II and III) at high elevations (Figs. 1 and 2). The overwhelming majority of zircons in these rivers are colorless. However, typical rivers have about 20% colored zircons, which is more than could be reasonable supplied by the thin strip of greywacke along the top of the drainage divide. Our data (unpublished) suggests that the base of the CRZ lies within the Biotite Zone, which in the central part of the Southern Alps is inferred to have experienced temperatures of ~ 320–370 °C (Grapes, 1995).

5.3. FT ages of detrital zircon

The detrital fission-track grain-age (FTGA) spectra for the Hokitika River (west-draining) and the Rangitata River (east-draining) are very different (Table 2; Fig. 7). The dominant population of grain ages (or "peak" ages) in the Rangitata River is ~ 154 Ma, with smaller populations at ~ 102 and 222 Ma. None of the zircons have been reset in the late Cenozoic and, therefore, all of these zircons appear to have been derived from the unreset FT color zone. Grain ages in the west-draining Hokitika River are between about 2 and 80 Ma and in this range two principal peak ages occur at ~ 6.5 Ma and ~ 73.0 Ma. About 90% of the detrital zircons in this suite occur in this range of grain ages (~ 2–80 Ma), while ~ 10% occur in an age range similar to those shed to the east. Detritus shed to the west side of the mountain belt clearly records a distinct thermochronologic signature of orogenesis.

6. Discussion

Above, we hypothesized that the integration of the two parameters of zircon FT age and zircon color when applied to an exhumed crustal section would allow the definition of at least three crustal layers or zones. Based on what we know about the crustal structure of the Southern Alps collision zone (e.g. Beaumont et al., 1996) together with the data presented here, we show a cross-section of the orogen the disposition of the three zircon FT-color zones (Fig. 5). Our data require that the base of the unreset FT color zone is located at or close to the Main Divide in the central part of the orogen, which is consistent with previously reported zircon FT data (Kamp et al., 1989; Tippett and Kamp, 1993). The two underlying zones are exhumed between the Main Divide and the Alpine Fault within the Alpine Schist belt (Fig. 1). Here, we estimate from our detrital data the proportion of grains derived from each of these two lower zones. The concepts underlying this paper, particularly the value for tectonic studies of integrating the FT and color signals in zircon, grew out of basic observations about color and FT age made for the detrital zircon samples analyzed as part of this study and attempts to explain the observations. However, the obvious next step is to analyze the color properties of zircon concentrates from basement samples collected across and along the orogen, which is ongoing for samples reported by Kamp et al. (1989) and Tippett and Kamp (1993).

The rapid and recent erosional exhumation of the crust beneath the Southern Alps, driven by the oblique collision of the Australia and Pacific plates, is a key factor in the preservation of distinctive zircon color zones, and FT-age pattern, as well as prograde metamorphic zones. The rapid onset of Late Miocene exhumation led to rapid cooling and fossilization of zones that had previously reached thermal equilibrium. The combined zircon color and FT zonation pattern will not be affected by the advection of geo-

therms in response to rock uplift as the zonation pattern is set when the rock section experienced maximum temperatures; once rock uplift and associated erosion starts, the rock section progressively cools.

What do the FT ages and the distribution of color in the detrital zircon data tell us about the relative proportion of eroded material from either the reset FT color zone (rFTCZ) or the reset FT colorless zone? If we can relate zircon color and FT ages in the modern setting, we can reconstruct how the Southern Alps and other orogenic belts were unroofed at the onset of deformation. Recall that east-draining rivers have an abundance of colored zircon, but they also have some colorless zircon (see Table 1). In the Rangitata River 60% of the zircons have color. The zircons in the west-draining Hokitika River are derived from the reset FT color zone and the reset FT colorless zone with a minor component derived from the unreset FT color zone (Fig. 5). A notable aspect of this FT grain-age distribution is that there is a wide range of grain ages < 80 Ma that reflect cooling events in the crustal section below the unreset FT color zone. Below the unreset FT color zone, ~20% of the zircons have significant color.

We estimate that about 60% of the zircon grains in the Hokitika River sample were derived from rocks that originally lay within the reset FT colorless zone. To make this estimate, we assume an original ratio of color:colorless grains for the Torlesse (~ 1.84 for the Rangitata River, see Table 1, red + yellow:colorless zircon percentage), and apply this to the Hokitika River sample. In this rough estimate, we assume that 21% of the zircons in the Hokitika have color and we would expect roughly 33% could have been from above the reset FT colorless zone (21% + 12% = 33%; recall that some zircons will not have color regardless of source) and about 67% which are colorless would, therefore, be from below the reset FT colorless zone. Turning to the FT data, we see that about 41% of the grains in the Hokitika sample have FT ages that are 73 Ma or older and about 60% of the zircons have FT ages that belong to the 21 Ma peak or younger. Although there is uncertainty in these calculations, we are struck by the fact that we can probably attribute the 60% of the grains < 21 Ma to the 67% that are colorless and presumably derived from below the reset FT colorless zone. If we take this a step farther, we would note that some fraction must have originally resided in the reset FT color zone and some fraction from the unreset FT color zone—the upper two crustal layers. The former fraction may have been represented by the grains that comprise the 73 Ma peak (32% see Table 2). Note that other workers have documented an interval between 68 and 81 Ma characterized by localized anatectic partial melting at depth (see Batt et al., 1999). It is likely that this event resulted in higher than normal heat flow and thermal resetting at higher levels. Finally, the remaining 9% of the zircon grains that belong to the ~ 149 Ma peak (and older) were probably derived from rocks that resided in the unreset FT color zone prior to the onset of exhumation. Recall that all of these zones contain colorless zircon, but only the upper two zones contain colored zircons. In the case outlined above, any grain with color must have been derived from one of the two upper crustal layers and, therefore, the FT age records exhumation of those particular layers.

A remarkable feature about the detrital zircon FT age data is that samples, one derived from the upper part of the crust and the other from the middle to lower crust, have captured the essential elements of the thermo-tectonic evolution of the Torlesse in this part of New Zealand. Torlesse provenance ages (230 Ma) eroded from the highest level crust are represented by component P3 in the Rangitata River sample. Component P1 at 100 Ma in the same sample represents the timing of a major Late Cretaceous cooling event widely recognised in the Torlesse basement (Kamp, 2001) and attributed to exhumation in the inboard parts of the contemporary accretionary prism. Component P2 in the Rangitata River sample having intermediate ages represents grains eroded from the ZPAZ fossilized by the 100 Ma cooling event and exhumed to the surface during the Late Cenozoic. The Hokitika sample comprises a much lower number of grains with Mesozoic ages, but elements of the Late Cretaceous ZPAZ and 100 Ma reset ages are present as well as the ca. 73 Ma peak associated with a Late Cretaceous thermal maxima outlined above (Fig. 7b). The P1 component centered on 6.5 Ma represents the timing of significant cooling/exhumation associated with the initiation of rock uplift that has resulted in the Late Cenozoic development of the Southern Alps as a major topographic

feature. The spread of Paleogene to mid-Neogene ages in the Hokitika sample represents the erosion of the Late Cenozoic ZPAZ. The capturing of all these events in just two strategically located samples attests to the thoroughness of mixing in fluvial environments even those of coarse braided character (see also Bernet et al., 2001). Based on these results, we are encouraged to apply the same technique to ancient sequences.

While it is clear that the color of zircon can be a useful gauge of its thermal history, more data are needed to better quantify the various aspects of zircon color. Several directions will be fruitful in this regard, but what is clearly needed is a better understanding of the temperature constraints of color removal over prolonged annealing conditions. Additionally, laboratory studies are needed to better constrain the rate of color removal and how individual grains progressively lose color. These studies should be tied to understanding the single-grain geochemistry and how the REE or other elements affect zircon color. Finally, experimental data on synthetically prepared zircon, doped with the REE and, subsequently, irradiated will help our understanding of which trace elements are primarily responsible for zircon color. Eventually, we suspect that the relationship between zircon chemistry, zircon color, and thermal history will be fully quantified and, in this case, color will be extremely useful in ceramic, petrogenetic, and tectonic studies.

Acknowledgements

We gratefully acknowledge the technical assistance of K. Ortel-Cass (zircon color), G. Xu (FT analysis), J.A. Smith (fieldwork), D.S. Pratt and B. Dodd (irradiation), and M. Roberts (template for zircon habits). This work was funded by the NSF grants EAR 9614730 and EAR 9418989 (to Garver) and the N.Z. Foundation for Research, Science, and the Technology grant UOW 507 (to Kamp). The Reactor Use Sharing (R.U.S.) program (US DOE) awarded to the Oregon State Reactor Facility funded irradiation, in part. This and earlier versions of this paper were improved by comments and suggestions by P. Copeland, T. Ireland, R.L. Fleischer, R. Ketcham, P.F. Green, and an anonymous reviewer.

References

Adams, C.J., Gabities, J.E., 1985. Age of metamorphism and uplift of the Haast Schist Group at Haast Pass, Lake Wanaka and Lake Hawea, South Island, New Zealand. N. Z. J. Geol. Geophys. 28, 85–96.

Batt, G., Kohn, E., Braun, B.P., McDougall, J., Irelend, T.R., 1999. New insight into the dynamic development of the Southern Alps, from detailed thermochronologic investigation of the Matake-take Range pegmatites. In: Ring, U., Brandon, M.T., Willett, S., Lister, G. (Eds.), Exhumation Processes: Normal Faulting, Ductile Flow, and Erosion. Geol. Soc. London, Spec. Publ., vol. 154, pp. 283–304.

Beaumont, C., Kamp, P.J.J., Hamilton, J., Fullsack, P., 1996. The continental collision zone, South Island, New Zealand: comparison of geodynamical models and observations. J. Geophys. Res. 101 (B2), 3333–3359.

Bernet, M., Zattin, M., Garver, J.I., Brandon, M.T., Vance, J.A., 2001. Steady state exhumation of the European Alps. Geology 29 (1), 35–38.

Brandon, M.T., 1996. Probability density plot for fission-track grain-age samples. Radiat. Meas. 26 (5), 663–676.

Brandon, M.T., Roden-Tice, M.R., Garver, J.I., 1998. Late Cenozoic exhumation of the Cascadia accretionary wedge in the Olympic Mountains, northwest Washington State. Geol. Soc. Am. Bull. 110, 985–1009.

Carter, A., Moss, S.J., 1999. Combined detrital-zircon fission-track and U–Pb dating: a new approach to understanding hinterland evolution. Geology 27 (3), 235–238.

Chakoumakos, B.C., Murakami, T., Lumpkin, G.R., Ewing, R.C., 1987. Alpha-decay-induced fracturing in zircon: the transition from the crystalline to the metamict state. Science 236, 1556–1559.

Coyle, D.A., Wagner, G.A., 1996. Fission-track dating of zircon and titanite from the 9101 m deep KTB: observed fundamentals of track stability and thermal history reconstruction. Paper Presented at the International Workshop on Fission Track Dating, University of Ghent, Ghent, Belgium, Aug. 26–30, 1996.

Deer, W.A., Howie, R.A., Zussman, J., 1982. Rock Forming Minerals, second ed. Orthosilicates., vol. 1A. Halsted, New York, 919 pp.

Ellsworth, S., Navrotsky, A., Ewing, R.C., 1994. Energetics of radiation damage in natural zircon ($ZrSiO_4$). Phys. Chem. Miner. 21, 140–149.

Ewing, R.C., 1994. The Metamict state: 1993—the centennial. Nucl. Instrum. Methods Phys. Res., Sect. B 91, 22–29.

Fielding, P.E., 1970. The distribution of uranium, rare earths, and color centers in a crystal of natural zircon. Am. Mineral. 55, 429–440.

Fleischer, R.L., Price, P.B., Walker, R.M., 1975. Nuclear Tracks in Solids Univ. California Press, Berkeley, CA, 605 pp.

Gaudette, H.E., Vitrac-Michard, A., Allègre, C.J., 1981. North American Precambrian history recorded in a single sample: high resolution U–Pb systematics of the Potsdam Sandstone detrital zircons, New York State. Earth Planet. Sci. Lett. 54, 248–260.

Garver, J.I., Brandon, M.T., 1994a. Fission-track ages of detrital

zircon from mid-Cretaceous sediments of the Methow–Tyaughton basin, southern Canadian Cordillera. Tectonics 13 (2), 401–420.

Garver, J.I., Brandon, M.T., 1994b. Erosional denudation of the British Columbia Coast Ranges as determined from fission-track ages of detrital zircon from the Tofino basin, Olympic Peninsula, Washington. Geol. Soc. Am. Bull. 106, 1398–1412.

Garver, J.I., Brandon, M.T., Roden-Tice, M., Kamp, P.J.J., 1999a. Erosional denudation determined by fission-track ages of detrital apatite and zircon. In: Ring, U., Brandon, M.T., Willett, S., Lister, G. (Eds.), Exhumation Processes: Normal Faulting, Ductile Flow, and Erosion. Geol. Soc. London, Spec. Publ., vol. 154, pp. 283–304.

Garver, J.I., Soloviev, A.V., Kamp, P.J.J., Brandon, M.T., 1999b. Detrital zircon fission track thermochronology: practical considerations and examples. Mem. Sci. Geol. (in English) 51, in press.

Garver, J.I., Soloviev, A.V., Bullen, M.E., Brandon, M.T., 2000. Towards a more complete record of magmatism and exhumation in continental arcs using detrital fission track thermochronmentry. Phys. Chem. Earth 25, 565–570.

Gastil, R.G., DeLisle, M., Morgan, J., 1967. Some effects of progressive metamorphism on zircons. Geol. Soc. Am. Bull. 78 (7), 879–906.

Gehrels, G.E., Dickinson, W.R., 1995. Detrital zircon provenance of Cambrian to Triassic miogeoclinal and eugeoclinal strata in Nevada. Am. J. Sci. 295 (1), 18–48.

Gehrels, G.E., Butler, R.F., Bazard, D.R., 1996. Detrital zircon geochronology of the Alexander terrane, southeastern Alaska. Geol. Soc. Am. Bull. 108, 722–734.

Grapes, R.H., 1995. Uplift and exhumation of Alpine Schist, Southern Alps, New Zealand: thermobarometric constraints. N. Z. J. Geol. Geophys. 38, 525–533.

Gray, M.B., Zietler, P.K., 1997. Comparison of clastic wedge provenance in the Appalachian foreland using U/Pb ages of detrital zircons. Tectonics 16 (1), 151–160.

Green, P.F., Hegarty, K.A., Duddy, I.R., Foland, S.S., Gorbachev, V., 1996. Geological constraints on fission track annealing in zircon. Paper Presented at the International Workshop on Fission-Track Dating, University of Ghent, Ghent, Belgium, August 26–30, 1996.

Hasebe, N., Tagami, T., Nishimura, S., 1993. Evolution of the Shimanto accretionary complex: a fission-track thermochronological study. In: Underwood, M.B. (Ed.), Thermal Evolution of the Tertiary Shimanto Belt, Southwest Japan: An Example of Ridge-Trench Interaction. Geol. Soc. London, Spec. Pap. vol. 273, pp. 121–136.

Hutton, C.O., 1950. Studies of heavy detrital minerals. Geol. Soc. Am. Bull. 61, 635–716.

Holland, H.D., Gottfried, D., 1955. The effect of nuclear radiation on the structure of zircon. Acta Crystallogr. 8, 291–300.

Ireland, T.R., 1992. Crustal evolution of New Zealand: evidence for age distributions of detrital zircons in Western Province paragneiss and Torlesse graywacke. Geochim. Cosmochim. Acta 56, 911–920.

Kamp, P.J.J., 2001. Possible Jurassic age for part of Rakaia Terrane in Canterbury: implications for the development of the Torlesse accretionary prism. N. Z. J. Geol. Geophys. 44, 185–203.

Kamp, P.J.J., Green, P.F., White, S.H., 1989. Fission track analysis reveals character of collisional tectonics in New Zealand. Tectonics 8, 169–195.

Kamp, P.J.J., Green, P.F., Tippett, J.M., 1992. Tectonic architecture of the mountain front-foreland basin transition, South Island, New Zealand, assessed by fission track analysis. Tectonics 11, 169–195.

Kasuya, M., Naeser, C., 1988. The effect of α-damage on fission track annealing in zircon. Nucl. Tracks Radiat. Meas. 14, 477–480.

Kodymová, A., 1977. Occurrence of pink (Archean?) zircon in the pre-Cambrian of central and Western Bohemia (in English; translated). Vestn. Ustred. Ustavu Geol. 52, 121–123.

Lonergan, L., Johnson, C., 1998. Reconstructing orogenic exhumation histories using synorogenic detrital zircons and apatites: an examples from the Betic Cordillera, SE Spain. Basin Res. 10, 353–364.

Miller, M.M., Saleeby, J.B., 1991. Continental detrital zircon in Carboniferous ensimatic arc rocks, Bragdon Formation, Eastern Klamath terrane, northern California. Geol. Soc. Am. Bull. 103, 268–276.

Murakami, T., Chakoumakos, B.C., Ewing, R.C., Lumpkin, G.R., Weber, W.J., 1991. Alpha-decay damage in zircon. Am. Mineral. 76, 1510–1532.

Naeser, N.D., Zeitler, P.K., Naeser, C.W., Cerveny, P.F., 1987. Provenance studies by fission-track dating—etching and counting procedures. Nucl. Tracks Radiat. Meas. 13, 121–126.

Nasdala, L., Wenzel, M., Vavra, G., Irmer, G., Wenzel, T., Kober, B., 2001. Metamictisation of natural zircon: accumulation versus thermal annealing of radioactivity-induced damage. Contrib. Mineral. Petrol. 141, 125–144.

Nerurkar, A.P., Reena, D.E., Chakraborty, P.N., Kaul, I.K., 1979. Studies on thermoluminescence, metamictization and sintering properties of zircon sands. Mod. Geol. 7, 13–24.

Pickard, A.L., Adams, C.J.D., Barley, M.E., 2000. Australian provenance for Upper Permian to Cretaceous rocks forming accretionary complexes on the New Zealand sector of the Gondwanaland margin. Aust. J. Earth Sci. 47, 987–1007.

Poldervaart, A., 1955. Zircons in rocks: 1. Sedimentary rocks. Am. J. Sci. 253, 433–461.

Poldervaart, A., 1956. Zircons in rocks: 2. Igneous rocks. Am. J. Sci. 254, 521–554.

Pupin, J.P., 1980. Zircon and granite petrology. Contrib. Mineral. Petrol. 73, 207–220.

Rainbird, R.H., McNicoll, V.J., Thériault, R.J., Heaman, L.M., Abbott, J.G., Long, D.F.G., Thorkelson, D.J., 1997. Pan-continental river system draining Grenville orogen recorded by U–Pb and Sm–Nd geochronology of Neoproterozoic quartzarenites and mudrocks, northwestern Canada. J. Geol. 105, 1–17.

Roback, R.C., Walker, N.W., 1995. Provenance, detrital U–Pb geochronometry, and tectonic significance of Permian to Lower Triassic sandstone in southeastern Quesnellia, British Columbia and Washington. Geol. Soc. Am. Bull. 107 (6), 665–675.

Schäfer, H-J., Gebauer, D., Naegler, T., Eguiluz, L., 1995. Conventional and ion-microprobe U–Pb dating of detrital zircons of the Tentudia Group (Serie Negra, SW, Spain): implications for zircon systematics, stratigraphy, tectonics, and the Precambrian/

Cambrian boundary. Contrib. Mineral. Petrol. 113 (3), 289–299.

Scott, D.J., Gauthier, G., 1996. Comparison of TIMS (U–Pb) and laser ablation microprobe ICP-MS (Pb) techniques for age determination of detrital zircons from Paleoprotozoic metasedimentary rocks from northeastern Laurentia, Canada, with tectonic implications. Chem. Geol. 131 (1–4), 127–142.

Sircombe, K.N., Kamp, P.J.J., 1998. The South Westland Basin: seismic stratigraphy, basin geometry and evolution of a foreland basin within the Southern Alps collision zone, New Zealand. Tectonophysics 300, 359–387.

Smith, M., Gehrels, G., 1994. Detrital zircon geochronology and provenance of the Harmony and Valmy formations, Roberts Mountain Allochthon, Nevada. Geol. Soc. Am. Bull. 106 (7), 968–979.

Speer, J.A., 1980. Zircon. In: Ribbe, P.H. (Ed.), Reviews in Mineralogy. Orthosilicates, vol. 5. Mineralogical Society of America, Washington, DC, pp. 67–112.

Tagami, T., Carter, A., Hurford, A.J., 1996. Natural long term annealing of the zircon fission-track system in Vienna Basin deep borehole samples: constraints upon the partial annealing zone and closure temperature. Chem. Geol. 130, 147–157.

Tagami, T., Galbraith, R.F., Yamada, R., Laslett, G.M., 1998. Revised annealing kinetics of fission tracks in zircon and geological implications. In: van den Haute, P., de Corte, F. (Eds.), Adv. Fission-Track Geochronol. Kluwer Academic Press, Norwell, MA, pp. 99–112.

Tippett, J.M., Kamp, P.J.J., 1993. Fission track analysis of the Late Cenozoic vertical kinematics of continental Pacific crust, South Island, New Zealand. J. Geophys. Res. 98, 16119–16148.

Tomita, T., Karakida, Y., 1954. Effects of heat on the color and structure of hyacinth from Mamutu, Formosa. Recent Prog. Nat. Sci. Jpn. (a.k.a. Nihon Shizen Kagaku Shuho) 25 (3–4), 145–153.

Weber, W.J., Ewing, R.C., Wang, L-M., 1994. The radiation-induced crystalline-to-amorphous transition in zircon. J. Mater. Res. 9, 688–698.

Woodhead, J.A., Rossman, G.R., Silver, L.T., 1991. The metamictization of zircon: radiation dose-dependent characteristics. Am. Mineral. 76, 74–82.

Zhao, J.X., McCulloch, M.T., Bennett, V.C., 1992. Sm–Nd and U–Pb zircon isotopic constraints on the provenance of sediments from the Amadeus basin, Central Australia: evidence for REE fractionation. Geochim. Cosmochim. Acta 56, 921–940.